

## Superconducting Interactions in Tin Telluride\*

J. K. HULM AND C. K. JONES

*Westinghouse Research Laboratories, Pittsburgh, Pennsylvania 15235*

AND

D. W. DEIS,† H. A. FAIRBANK,† AND P. A. LAWLESS†

*Duke University, Durham, North Carolina 27706*

(Received 8 December 1967)

The range of superconductivity in tin telluride has been extended down to  $4 \times 10^{20}$  carriers per cc. Experimentally there is no indication of a cutoff in superconductivity, although the data are not inconsistent with the theoretically indicated cutoff at  $4 \times 10^{19}$  carriers per  $\text{cm}^3$ . By using a modified form of the Morel-Anderson theory in conjunction with a modified BCS equation due to McMillan, it is possible to fit the experimental data and to find the magnitude of the umklapp contribution to the attractive phonon interaction. The resulting values are approximately a factor of 10 smaller than the values predicted by the Morel-Anderson theory.

## INTRODUCTION

THE general success of the BCS theory<sup>1</sup> in providing a quantitative calculation of many superconducting properties relative to the normal state has, unfortunately, not so far included the most obvious and first measured parameter of a superconductor, its critical temperature  $T_c$ . This difficulty does not lie in any basic failure of the theory but rather in the problem of calculating, with sufficient accuracy, the superconducting interaction energy. In the BCS model the critical temperature is expressed relative to the lattice phonon temperature in terms of an exponential function of the inverse net interaction energy. A change of the interaction energy by a factor of 2 may change the critical temperature by one or two orders of magnitude, which greatly complicates the problem of a precise calculation of  $T_c$ .

In the primitive BCS theory no attempt was made to calculate the interaction energy in detail. Instead, the net potential, the difference between the phonon attractive energy and the Coulomb repulsion energy, was represented by a single parameter  $V$ . Later Morel and Anderson<sup>2</sup> carried out a detailed calculation of the components of  $V$  using a jellium model with screening and including retardation effects. Morel and Anderson considered the contributions of both normal and umklapp processes, although the latter interactions were not evaluated in detail. The umklapp model, assumed valid for polyvalent materials, was used to estimate the isotope effect in the metallic elements, with indifferent success. Perhaps this is not surprising in view of the extensive simplifying assumptions of the model and the

uncertainties regarding the real magnitude of the umklapp contribution.

The results of Morel and Anderson's calculations appear primarily as a function of the free-electron density of the jellium. In metals, of course, this parameter is limited to a relatively narrow range in the vicinity of  $10^{23}$  electrons per  $\text{cm}^3$ . In semimetals or heavily doped semiconductors, however, a much larger range of carrier densities is possible, extending from  $10^{23}$  down to almost any desired value. We discovered superconductivity about five years ago in this class of materials.<sup>3</sup> The first superconductors of this type were the rocksalt-structure tellurides of germanium and tin<sup>4</sup> with nominal compositions GeTe and SnTe, respectively. In preliminary experiments  $p$ -type samples of these compounds doped by a slight germanium or tin deficiency were found to be superconducting at about 0.1°K, for hole densities in the neighborhood of  $10^{21}$  per  $\text{cm}^3$ . In this paper we report on a more detailed investigation of the critical temperature as a function of carrier concentration  $n$  as the latter is varied by a factor of about 20. This has enabled us to carry out a more detailed comparison with theory than was heretofore possible.

Although initial experiments were concerned with GeTe, serious metallurgical difficulties were encountered with this compound. Owing to a slight rhombohedral distortion of the cubic lattice which occurs in GeTe as the material is cooled through 300°C, a very complex domain structure is formed. This gives rise to a wide variation in local strain in the sample, and hence the superconducting results are highly dependent upon the exact thermal history. Thus far we have been unable to systematize this behavior.

<sup>3</sup> R. A. Hein, J. W. Gibson, R. Mazelsky, R. C. Miller, and J. K. Hulm, *Phys. Rev. Letters* **12**, 230 (1964).

<sup>4</sup> R. A. Hein, J. W. Gibson, R. S. Allgaier, B. B. Houston, Jr., R. Mazelsky, and R. C. Miller, in *Proceedings of the Ninth International Conference on Low-Temperature Physics, Columbus, Ohio*, edited by J. A. Daunt *et al.* (Plenum Press, Inc., New York, 1965), p. 604.

\* Work supported in part by the Army Research Office, Durham, N.C.

† Supported in part by the National Science Foundation.

<sup>1</sup> J. Bardeen, L. N. Cooper, and J. R. Schrieffer, *Phys. Rev.* **108**, 1175 (1957).

<sup>2</sup> P. Morel and P. W. Anderson, *Phys. Rev.* **125**, 1263 (1962).

Preliminary experiments on the sister compound SnTe showed that reproducible superconducting data could be obtained irrespective of the exact annealing procedure employed. These results are consistent with the view that there is no structural anomaly in this compound. SnTe was therefore chosen as the material for a thorough investigation of the  $T_c$ - $n$  relationship.

Tunneling measurements<sup>5</sup> have shown that SnTe is a semiconductor with an energy gap of 0.3 eV at 4.2°K. Measurements of the Seebeck coefficient<sup>6</sup> indicate that there are two valence bands with different energies. Even though SnTe can be classed as a semiconductor, in the range of carrier densities used in this work it behaves more as a dilute metal, having a nearly temperature-independent Hall coefficient and a positive electrical conductivity coefficient.

In the present work only  $p$ -type SnTe was investigated. Doping was carried out in two essentially different ways; first, the creation of tin vacancies by varying  $x$  in the formula  $\text{Sn}_{1-x}\text{Te}$ , and second, the substitution of various nondivalent impurities for tin. Hole densities from about  $2 \times 10^{21}$  per  $\text{cm}^3$  down to  $1 \times 10^{20}$  per  $\text{cm}^3$  were studied with critical temperatures ranging from about 0.2°K to below 15 m°K. The results are analyzed in terms of a modified form of Morel and Anderson's expressions for the interaction energies and employing a modified BCS relationship due to McMillan<sup>7</sup> connecting the interaction energy with the critical temperature. From these considerations we conclude that at low carrier densities normal processes give the major contribution to the attractive interaction, and that the small umklapp contribution necessary to explain the results is at least an order of magnitude less than theoretically predicted.

## EXPERIMENTAL

### Samples

All samples employed in this investigation were prepared by sintering techniques. The appropriate amounts of the constituents for a sample of approximately 4 g weight were weighed out to within 0.1 mg, sealed into an evacuated fused quartz tube and melted by heating overnight at 900°C. The melt was then homogenized by continuous agitation on removal from the furnace until solidification occurred on cooling. On removal from the tube the ingot was crushed, and ground to an approximately 200-mesh particle size using an agate mortar and pestle to minimize the possibility of contamination. The powder was then compacted in a split tungsten carbide die into cylinders, typically 0.220-in. diam and 1-in. long, using a compacting pres-

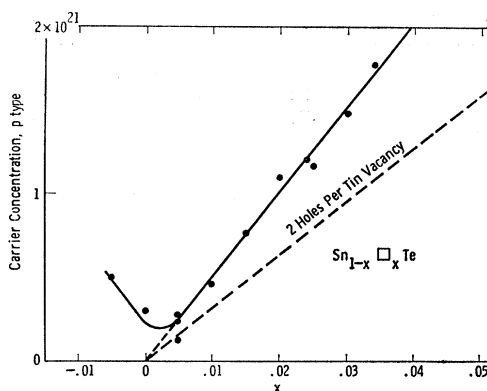


FIG. 1. Nominal carrier density of  $\text{Sn}_{1-x}\text{Te}$  as a function of tin deficiency.

sure between 5000 and 7000 psi. Each cylinder was sealed into an evacuated quartz tube and sintered at 500°C for 3–4 days. A sample of standard geometry  $\frac{1}{8}$  in.  $\times$   $\frac{1}{8}$  in.  $\times$   $\frac{1}{2}$  in. was then cut from the center of the cylinder. In a few representative cases, excess material adjacent to the sample was crushed and the composition checked by x-ray lattice parameter determination.<sup>8</sup> This measurement was carried out using a Norelco Debye-Scherrer powder camera of 57.3-mm radius employing copper  $K\alpha$  radiation at 35 kV and 20 mA. The Taylor extrapolation function was employed to correct for absorption. For the most part, x-ray determined composition agreed well with the nominal chemical composition.

In our work the carrier densities were estimated from measurements of the low-field Hall constant at 77°K. As already mentioned, one source of carriers in SnTe is a departure from stoichiometry. As the stoichiometric compound is approached, the carrier density goes to zero, suggesting that if the normal ionic valence of  $-2$  is assumed for tellurium the tin must appear as a  $+2$  ion thereby yielding two carriers (holes) for every tin vacancy. In Fig. 1, the carrier density of  $\text{Sn}_{1-x}\text{Te}$  from Hall-effect measurements is plotted as a function of tin deficiency and suggests that about three carriers are present for every tin vacancy instead of the expected value of 2. This agrees with the earlier work of Mazelsky and Lubell,<sup>8</sup> and the discrepancy can perhaps be attributed to complexities in the band structure of SnTe which invalidate our simple, direct interpretation of the Hall data.

Starting with a sample with a high tin deficiency, the hole concentration can be reduced by doping with impurities. In this work, arsenic and antimony were used to dope a  $\text{Sn}_{0.970}\text{Te}$  sample having a nominal carrier density of  $14.9 \times 10^{20}$  carriers per  $\text{cm}^3$ . The decrease in the hole concentration as a function of the

<sup>5</sup> L. Esaki and P. J. Stiles, Phys. Rev. Letters **16**, 1108 (1966).

<sup>6</sup> J. A. Kafalas, R. B. Brebrick, and A. J. Strauss, Appl. Phys. Letters **4**, 93 (1964).

<sup>7</sup> W. L. McMillan, Phys. Rev. **167**, 331 (1968).

<sup>8</sup> R. Mazelsky and M. S. Lubell, Advan. Chem. Ser. **39**, 210 (1963).

TABLE I. Electrical data for metallic NaCl-structure compounds.

Compound	Type	Carrier density $\text{cm}^{-3}$	Resis- tivity (298°K) $\mu\Omega \text{ cm}$	Resis- tivity (4°K) $\mu\Omega \text{ cm}$	$T_c$ °K
SnAs	<i>n</i>	$1.4 \times 10^{22}$	20.8	3.0	$3.5 \pm 0.2^\circ$
SnSb	<i>n</i>	$2.9 \times 10^{22}$	26.0	11.0	$1.6 \pm 0.05^\circ$

amount of impurity present is shown in Fig. 2. The behavior upon addition of antimony is consistent with the antimony occupying vacant tin sites with a valence of +5, thereby yielding 3 excess electrons for every antimony present. This should lead to full compensation at 1.2 at.% antimony as shown in Fig. 2. The less rapid compensation of arsenic is harder to explain but could be accounted for by taking a lower valence for arsenic such as +3, or by locating some of the arsenic atoms on tellurium sites with a -5 valence where they would act as donors.

As can be seen in Fig. 2, there is a definite break point for both doped compounds where they become two phase. The two-phase system would be a mixture of tin arsenide or tin antimonide with tin telluride. Both tin arsenide and tin antimonide have a rocksalt structure like tin telluride but are only slightly soluble in tin telluride.

For arsenic and antimony contents around 10% and higher we were able to detect a superconducting transition due to the second phase, SnAs or SnSb. Both of these compounds were found to be essentially metallic with the characteristics shown in Table I. The solubility of tellurium in both compounds is apparently quite small. Thus, in the system  $(\text{SnAs})_{1-x}(\text{Sn}_{0.97}\text{Te})_x$ ,  $T_c$  remained constant at about 3.6°K as  $x$  was increased from 0 to 0.9 (Fig. 3). Beyond this composition there was a region of nonsuperconducting behavior followed by the reappearance of superconductivity at a much lower temperature, corresponding to single-phase doped SnTe. The behavior of  $(\text{SnSb})_{1-x}(\text{Sn}_{0.97}\text{Te})_x$  alloys was broadly similar (Fig. 3). Since the main object of our work was to test the  $T_c$ - $n$  relationship for SnTe itself, the doped samples discussed in the remainder of this paper were selected from the single-phase region.

#### Transition-Temperature Measurements

The superconducting transition temperature of tin telluride for all compositions studied so far lies below 0.3°K. It was therefore necessary to employ the technique of adiabatic demagnetization of a paramagnetic salt in order to achieve temperatures in this range. Two independent experimental systems were used in this work, one at the Westinghouse Research Laboratories and the other at Duke University.

The Westinghouse cryostat used single-stage demagnetization from a starting temperature of 1.2°K. With a chromalum salt pill and an initial field of 30 000 Oe a minimum temperature of 0.030°K was achieved. The Duke University cryostat was considerably more sophisticated, using He<sup>3</sup> cooling to give a starting temperature near 0.4°K and two-stage demagnetization. A minimum temperature near 0.013°K was obtained in this apparatus. Both cryostats employed superconducting solenoids to provide the required magnetizing fields. Thermal contact between the cooling salt pill and samples was attained by means of a pigtail of a large number (typically 200) of fine (30 gauge) high-purity copper wires into which the samples were cemented with GE 7031 lacquer. It was established in independent experiments that internal temperature gradients in the system in no case exceeded 0.001°K. The experimental volume containing the CMN thermometer and samples (up to five in a typical run) was magnetically shielded from the external fields (due to the magnet, etc.) by a composite system utilizing both superconducting and high-permeability materials. It was established that the resultant field seen by the samples was always below 0.010 Oe.

The techniques of measurement were essentially the same for both systems. In all cases the temperature of the transition was determined from a magnetic temperature scale using cerium magnesium nitrate (CMN) as the thermometric element, either in single-crystal or powdered form. The temperature scale was established by means of a Curie plot of the salt ac susceptibility versus inverse temperature at high temperatures which was linearly extrapolated into the range of interest. The transition from the normal to superconducting state or vice versa was detected via the abrupt change in ac penetration depth at this point. All magnetic measurements were carried out at frequencies between 17 and 150 cps employing a very sensitive modification

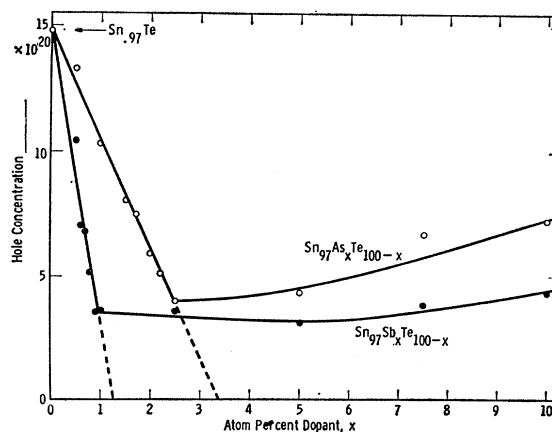


FIG. 2. Nominal carrier density of  $\text{Sn}_{0.97}\text{Te}$  as a function of impurity concentration.

of the ac Hartshorn mutual inductance bridge with synchronous detection. A peak field magnitude of 0.1 Oe was used for measurement of the CMN susceptibility and about 0.01 Oe for the detection of the superconducting transition.

The transitions were studied in detail while the experimental system warmed up at a convenient rate after cooling by demagnetization to the lowest temperature. The warming rate could be adjusted by the

TABLE II. Transition temperature data for self- and impurity-doped tin telluride.

Sample	Composition	Carrier density ( $10^{20} \text{ cm}^{-3}$ )	$T_c$ ( $\text{m}^\circ\text{K}$ )
a	SnTe (crystal)	20.0	207
a	SnTe (crystal)	16.9	168
a	SnTe (crystal)	12.8	100
a	SnTe (crystal)	10.5	65
G016A	$\text{Sn}_{0.965}\text{Te}$	13.4	168
G015A	$\text{Sn}_{0.975}\text{Te}$	11.7	165
G006	$\text{Sn}_{0.966}\text{Te}$	17.9	167
G007	$\text{Sn}_{0.976}\text{Te}$	12.1	125
G143	$\text{Sn}_{0.970}\text{Te}$	14.8	155
G383	$\text{Sn}_{0.980}\text{Te}$	10.5	92
G396a	$\text{Sn}_{0.985}\text{Te}$	6.75	48.5
G396b	$\text{Sn}_{0.985}\text{Te}$	6.75	43.3
G384	$\text{Sn}_{0.985}\text{Te}$	7.64	48
G329	$\text{Sn}_{0.990}\text{Te}$	5.06	28.5
G385	$\text{Sn}_{0.990}\text{Te}$	4.63	24
G328	$\text{Sn}_{0.995}\text{Te}$	2.98	13.8 <sup>b</sup>
G319	$\text{Sn}_{0.97}\text{As}_{0.005}\text{Te}_{0.995}$	13.3	108
G320	$\text{Sn}_{0.97}\text{As}_{0.010}\text{Te}_{0.990}$	10.9	73
G360	$\text{Sn}_{0.97}\text{As}_{0.015}\text{Te}_{0.985}$	8.03	51
G388	$\text{Sn}_{0.97}\text{As}_{0.017}\text{Te}_{0.983}$	7.52	58
G361	$\text{Sn}_{0.97}\text{As}_{0.020}\text{Te}_{0.980}$	5.9	31.8
G389	$\text{Sn}_{0.97}\text{As}_{0.022}\text{Te}_{0.978}$	5.08	33.2
G303	$\text{Sn}_{0.97}\text{As}_{0.025}\text{Te}_{0.975}$	4.02	13.8 <sup>b</sup>
G317	$\text{Sn}_{0.97}\text{Sb}_{0.005}\text{Te}_{0.995}$	10.4	68
G362	$\text{Sn}_{0.97}\text{Sb}_{0.006}\text{Te}_{0.994}$	7	48
G390	$\text{Sn}_{0.97}\text{Sb}_{0.007}\text{Te}_{0.993}$	6.83	38
G363	$\text{Sn}_{0.97}\text{Sb}_{0.008}\text{Te}_{0.992}$	5.13	22
G391	$\text{Sn}_{0.97}\text{Sb}_{0.009}\text{Te}_{0.991}$	3.53	19.5 <sup>b</sup>
G318	$\text{Sn}_{0.97}\text{Sb}_{0.010}\text{Te}_{0.990}$	3.65	23 <sup>b</sup>

<sup>a</sup> Reference 4.

<sup>b</sup> Indicates nonsuperconducting to the lowest temperature achieved.

judicious use of a built-in heater. The transition was either displayed automatically as a function of time on a strip-chart recorder or else plotted point by point versus temperature directly.

## RESULTS AND DISCUSSION

### Data

The results of the  $T_c$  measurements for both self-doped and impurity-doped SnTe are summarized in

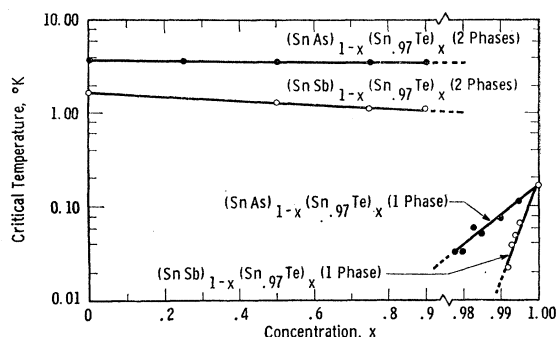


FIG. 3.  $T_c$  versus composition, alloys of  $\text{Sn}_{0.97}\text{Te}$  with SnAs and SnSb. (Note scale change on composition axis.)

Table II. The transition temperature was taken to be the point where the sample susceptibility reached one-half of its full diamagnetic value.

Several experiments were made to test the reproducibility of the data. For example, sample G396 was prepared in the same manner as the others but was larger in size, being  $\frac{1}{2}$  in. in diam by  $\frac{1}{2}$  in. long. Two smaller pieces were cut from this sample; one, G396a, was a  $\frac{1}{8}$ -in.-diam cylinder, and another, G396b, was a  $\frac{1}{8}$ -in.-square bar. The Hall-coefficient measurement was made on sample G396b and was assumed to apply for both samples. As Table II indicates, there was a noticeable difference of transition temperature between these two samples which we ascribe to slight concentration inhomogeneities in the original sample.

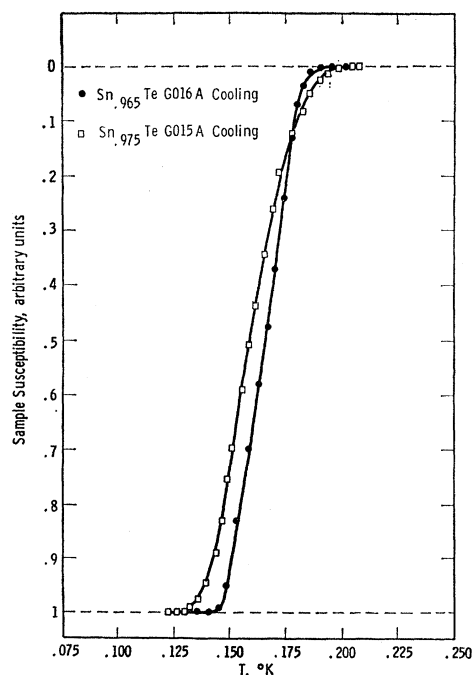


FIG. 4. Susceptibility versus temperature for two tin telluride samples showing broad transitions due to sample inhomogeneities.

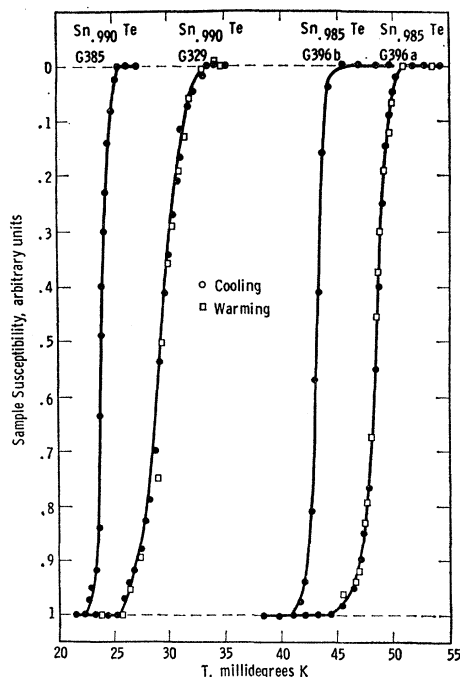


FIG. 5. Representative susceptibility-versus-temperature curves for four tin telluride samples having low transition temperatures.

$T_c$  measurements for samples G015A and G016A were made on  $\frac{1}{8}$ -in.-square pieces,  $\frac{1}{2}$  in. long, but these pieces were both cut from much larger samples, 1 in. diam and 2 in. long, which were prepared for heat-capacity measurements. Presumably because it is difficult to achieve good homogeneity in large samples, these specimens were found to exhibit rather broad transitions as shown in Fig. 4, and the  $T_c$  values were excluded from the final analysis. However, the majority of samples, which were prepared as  $\frac{1}{8}$ -in.-diam cylinders, exhibited quite narrow transitions of the type shown in Fig. 5. No difference in transition behavior could be detected between the self-doped samples shown in Fig. 5 and the impurity-doped samples.

From run to run the temperature values were apparently reproducible to about 5%, as estimated from repeated measurements of  $T_c$  for a given sample. For an intercomparison between the two laboratories involved,  $T_c$  for samples G360 and G362 were measured both at Duke and Westinghouse. The two sets of measurements agreed to within 0.5 mdeg, which is probably better than we have a right to expect.

The data of Table II are plotted in Fig. 6, from which a number of interesting features emerge. First, the scatter is somewhat larger than might be expected from temperature or carrier-density measurement errors, and is most likely due to appreciable inhomogeneities within the samples. Second, there is no evidence of a cutoff of  $T_c$  with decreasing carrier density, as was suggested in earlier, incomplete work.<sup>4</sup> Third,

there is no evidence of a maximum of  $T_c$  with increasing  $n$ , of the type which has been attributed to screening in the case of reduced strontium titanate.<sup>9</sup>

### Theory Used

We shall analyze the above data in terms of Morel and Anderson's<sup>2</sup> extension of the BCS model,<sup>1</sup> with modifications due to McMillan.<sup>7</sup> Morel and Anderson employed a screened Coulomb potential where the screening radius was determined by using a jellium model to characterize the solid. The retardation of the phonon interaction was included by solving the problem in terms of the Gor'kov-Eliashberg field theory.<sup>10,11</sup> In the modified form due to McMillan,<sup>7</sup>  $T_c$  is given by

$$T_c = \frac{\Theta_D}{1.45} \exp \left[ - \frac{1.04(1+\lambda)}{\lambda - \mu^*(1+0.62\lambda)} \right], \quad (1)$$

where  $\lambda$  represents the attractive phonon contribution to the interaction and  $\mu^*$  the repulsive Coulomb contribution. The parameter  $\lambda$  is given by

$$\lambda = \int_0^1 \frac{a^2}{a^2 + q^2/4k_0^2} x dx, \quad (2)$$

where

$$a^2 = k_s^2/4k_0^2, \quad (3)$$

$$x = |\bar{k}' - \bar{k}|/2k_0. \quad (4)$$

$k$  and  $q$  are electron and phonon wave vectors, respectively,  $k_0$  is the radius of the Fermi sphere, and  $k_s$  is the Fermi-Thomas screening radius. In Eq. (2) we have deviated slightly from Morel and Anderson by using the full dispersion relation for the velocity of sound as suggested by de Gennes.<sup>12</sup>

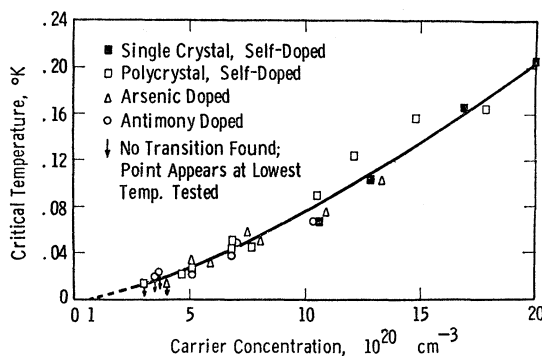


FIG. 6. Transition temperature of tin telluride samples as a function of carrier density. The single-crystal samples were grown from the melt rather than being prepared by sintering techniques.

<sup>9</sup> J. F. Schooley, W. R. Hosler, E. Ambler, J. H. Becker, M. L. Cohan, and K. C. Koonce, Phys. Rev. Letters **14**, 305 (1965).

<sup>10</sup> L. P. Gor'kov, Zh. Eksperim. i Teor. Fiz. **34**, 735 (1958) [English transl.: Soviet Phys.—JETP **7**, 505 (1958)].

<sup>11</sup> G. M. Eliashberg, Zh. Eksperim. i Teor. Fiz. **38**, 966 (1960) [English transl.: Soviet Phys.—JETP **11**, 696 (1960)].

<sup>12</sup> P. G. de Gennes, in *Superconductivity of Metals and Alloys* (W. A. Benjamin Inc., New York, 1966), p. 104.

For normal processes Eq. (4) reduces to  $x=q/2k_0$  and  $\lambda$  can be calculated directly as

$$\lambda_N = (a^2/2) \ln[(1+a^2)/a^2]. \quad (5)$$

Finding  $\lambda$  for umklapp processes is more difficult. Morel and Anderson assumed that  $q^2$  can be replaced by an average over the first Brillouin zone taking a quasispherical zone structure. This yields  $q^2=3q_D^2/5$  and thus

$$\lambda_U = \frac{1}{2} \left[ \frac{a^2}{a^2 + \frac{3}{5}(N/4n)^{2/3}} \right], \quad (6)$$

where  $N$  is the density of unit cells and  $n$  is the carrier density. By considering the relative sizes of the Fermi sphere and the first Brillouin zone it appears that at low carrier densities  $\lambda_N$  should be the important component in the attractive interaction, while at higher carrier densities  $\lambda_U$  should dominate.

The Coulomb repulsion parameter  $\mu^*$  in Eq. (1) is given by

$$\mu^* = \frac{\mu}{1 + \ln(\epsilon_F/\hbar\omega_1)}, \quad (7)$$

where  $\epsilon_F$  and  $\hbar\omega_1$  are the electron and phonon energies, respectively, and

$$\mu = (a^2/2) \ln[(1+a^2)/a^2]. \quad (8)$$

In order to use Eq. (1) to estimate  $T_c$  for a particular material we obviously need to know  $\lambda$ ,  $\mu^*$ , and  $\Theta_D$ . The interaction parameters  $\lambda$  and  $\mu^*$  may be obtained from Eqs. (5)–(8), providing the lattice parameter, the Fermi energy, and the screening parameter  $a$  are all known. These last two quantities may be derived on a quasi-free-electron model, in which case  $a^2$  is given by

$$a^2 = 1.945 \times 10^7 (m^*/mn^{1/3}). \quad (9)$$

The effective-mass ratio  $m^*/m$  is most readily obtained from measurements of the low-temperature heat capacity as a function of carrier density, using the

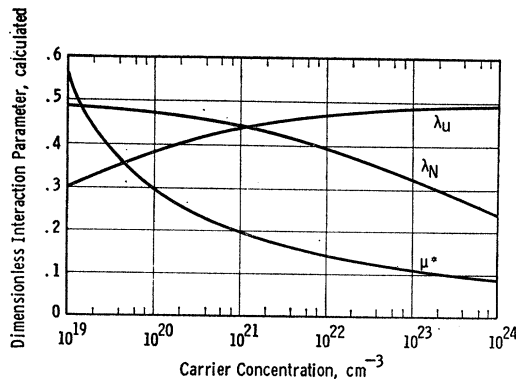


FIG. 7. Dimensionless interaction parameters (calculated) as a function of carrier density.

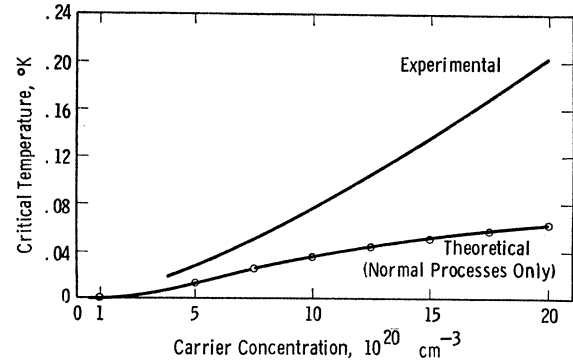


FIG. 8. Comparison of observed and theoretical transition temperatures in tin telluride.

expression for the electronic heat-capacity coefficient

$$\gamma = 0.136 (m^*n^{1/3}V_m/mN_A^{1/3}) \text{ mJ mole}^{-1} \text{ deg}^{-2}, \quad (10)$$

where  $V_m$  is the molar volume and  $N_A$  is Avagadro's number.

$\Theta_D$  may be derived from the lattice (cubic) term in the low-temperature heat capacity and  $\hbar\omega_1$  in Eq. (7) may be approximated by  $k\Theta_D$ .

#### Analysis of SnTe Data

In the region of interest the lattice parameter of SnTe varies from 6.302 Å ( $\text{Sn}_{0.97}\text{Te}$ ) up to 6.328 Å (SnTe).<sup>8</sup> A mean value of 6.315 Å was adopted in the present calculation, yielding a molar volume of 37.9 cc. From heat-capacity data<sup>13,14</sup>  $\Theta_D$  is 141°K and  $m^*/m$  is estimated at 1.706. Using these quantities the expected variation of  $\lambda_N$ ,  $\lambda_U$ , and  $\mu^*$  with carrier concentration for SnTe is shown in Fig. 7. The qualitative features of these curves with increasing  $n$ , i.e., the steep decrease of  $\mu^*$ , the gradual decrease of  $\lambda_N$ , and the slow rise of  $\lambda_U$  are general features to be expected for all superconductors on the particular model under discussion. If we would allow the other parameters such as  $\Theta_D$ ,  $m^*/m$  and the cell dimension to fluctuate over the entire range of variation of such parameters in nature, only slight displacements of these interaction strength curves would occur.

Physically the downtrend of  $\lambda_U$ , as we go to lower and lower carrier density, is quite sensible in view of the shrinkage of the Fermi sphere relative to the first Brillouin zone. As a first approach to this interpretation of our SnTe data, we therefore decided to ignore  $\lambda_U$  and to estimate  $T_c$  using  $\lambda_N$  and  $\mu^*$  alone. The results are shown in Fig. 8, where it will be seen that although the theoretical  $T_c$  curve rises with increasing  $n$ , in agreement with experiment, the theoretical estimates are too low and furthermore the theoretical curve shows an

<sup>13</sup> L. Finegold, J. K. Hulm, R. Mazelsky, N. E. Phillips, and B. B. Triplett, Ann. Finn. Acad. Sci., Ser. A6, 129 (1966).

<sup>14</sup> N. E. Phillips, J. K. Hulm, and C. K. Jones (to be published).

TABLE III. Estimated values of the attractive interaction parameter and its normal and umklapp components.

$n$ ( $10^{20}$ $\text{cm}^{-3}$ ) <sup>a</sup>	$T_c$ <sup>a</sup> °K	$\mu^*$ <sup>b</sup>	$\lambda$ <sup>c</sup>	$\lambda_N$ <sup>b</sup>	$\lambda - \lambda_N$	$\lambda_U$ <sup>b</sup>
5	0.027	0.221	0.473	0.452	0.0207	0.423
7.5	0.05	0.207	0.470	0.446	0.0231	0.432
10	0.076	0.199	0.470	0.442	0.0283	0.438
12.5	0.105	0.192	0.473	0.438	0.0346	0.442
15	0.136	0.187	0.476	0.435	0.041	0.446
17.5	0.168	0.183	0.479	0.432	0.0474	0.448
20	0.204	0.180	0.484	0.429	0.0544	0.450

<sup>a</sup> Experimental data from smoothed curve (Fig. 5).

<sup>b</sup> Theoretical estimates from Eqs. (5)–(9).

<sup>c</sup> Estimated from Eq. (1), using experimental  $T_c$ ,  $\Theta_D$ , and theoretical  $\mu^*$ .

obvious trend towards saturation due to the screening reduction of  $\lambda_N$  with increasing  $n$ .

It might be thought from Fig. 8 that a major correction to the interaction parameter would be necessary to bring the theory into agreement with experiment. Actually this is not the case, because the exponential dependence of  $T_c$  upon  $\lambda - \mu^*$  [Eq. (1)] causes  $T_c$  to be very sensitive to small changes of  $\lambda$ . As a matter of fact, if  $\lambda_N$  was increased about 10% over the Fig. 7 estimate, mainly at the higher carrier concentrations, this would be sufficient to raise the theoretical curve in Fig. 8 up to the experimental level. One possibility, therefore, is that the discrepancy of Fig. 8 can be blamed upon insufficient accuracy in our theoretical technique for estimating  $\lambda_N$ . It is quite surprising that a theory containing as many simplifying assumptions as those used in the Morel and Anderson model is capable of giving such good agreement with experiment as is demonstrated in Fig. 8.

An alternative possibility which seems more attractive to us is that the  $\lambda_N$  calculation is reasonably good

and that the occurrence of  $T_c$  values well above the normal-process theoretical curve is indicative of additional coupling due to the umklapp mechanism. We may in fact estimate the value of  $\lambda_U$  which must be added to  $\lambda_N$  in order to raise the estimated  $T_c$  up to the experimental curve in Fig. 8. This estimated  $\lambda_U$  is shown in Table III. As noted above, it is only about 10% of both  $\lambda_N$  and the theoretical  $\lambda_U$  obtained from Eqs. (7) and (8). We have no explanation of this discrepancy at the present time.

From Eq. (1) it can be shown that when  $\mu^* = \lambda(1 + 0.62\lambda)^{-1}$  there is a cutoff in transition temperature. If  $\lambda_U$  is neglected this cutoff occurs at  $n = 4 \times 10^{19}$  carriers per  $\text{cm}^3$  (Fig. 7). The experimental data is not inconsistent with this prediction, although it cannot be concluded from the data alone that there is a cutoff. It would certainly be an interesting test of the theory to examine other semiconductors at very low temperatures in order to check this prediction.

## CONCLUSION

We have observed that in the range of carrier concentration from  $4 \times 10^{20}$  to  $2 \times 10^{21}$  carriers per  $\text{cm}^3$ , the superconducting transition temperature of SnTe is a monotonically increasing function of carrier density and exhibits no sign of the saturation effects which might be expected on theoretical grounds due to screening of normal interaction processes by the surrounding electron gas. If the theory of the normal processes is assumed correct, it appears that there is an additional contribution to the BCS interaction due to umklapp processes. However, we note that our estimate of this additional component is about an order of magnitude lower than that predicted by Morel and Anderson's theory.

## ACKNOWLEDGMENTS

We wish to thank A. Foley and P. J. Steve for valuable help with these experiments, and R. C. Miller for numerous helpful discussions.